

# **How Do Ovarian Follicles Interact? A Many-Body Problem with Unusual Symmetry and Symmetry-Breaking Properties**

**H. Michael Lacker<sup>1</sup> and Allon Percus<sup>2,3</sup>**

*Received February 19, 1991*

---

The assumption that hormonal feedback regulates ovarian follicle growth is used to formulate a many-body problem in which interactions are spatially independent. This mechanism of interaction is shown to be sufficient to account for the regulation of ovulation number. A method is also developed to test if this assumption is consistent with the observed spatial distribution of follicles in the Rhesus monkey ovary.

---

**KEY WORDS:** Hormonal feedback; regulation of ovulation number; temporal self-organizing biological systems; follicular atresia; gradient systems of ordinary differential equations; physical systems with symmetry-breaking properties; polydisperse systems of soft spheres; Monte Carlo simulation.

## **1. INTRODUCTION**

Many-body problems where interactions are not spatially dependent are rare in physics and chemistry. In the endocrine system, however, spatially-independent many-body interaction arises in a natural way. Here chemical cell-to-cell signaling is mediated through hormones and a commonly shared circulation rather than by short-range diffusion. This can lead to an unusual degree of symmetry in the equations that describe the interaction. In higher vertebrates this is exemplified by the hormonal feedback system which controls the number of ovarian follicles that periodically reach full

---

<sup>1</sup> Departments of Biomathematical Sciences and Physiology & Biophysics, Mount Sinai School of Medicine, New York, New York 10029.

<sup>2</sup> Department of Physics, Harvard University, Cambridge, Massachusetts 02138.

<sup>3</sup> Present address: Niels Bohr Institute, University of Copenhagen, DK-2100 Copenhagen, Denmark.

maturity at the time of ovulation. This feedback system is primarily responsible for regulating the litter sizes that are characteristic for each mammalian species or breed. The observation that ovulation number per cycle is unchanged after an ovary is surgically removed suggests that this number is under physiological control. In fact, it has been repeatedly demonstrated in several mammalian species that ovulation number per cycle is nearly independent of the amount of ovarian tissue removed or the timing of its removal.<sup>(1,2)</sup>

The interacting units in the many-body problem that we will consider are developing ovarian follicles. A large reservoir of follicles is formed early in embryonic life. Initially each follicle is a spherical structure consisting of an egg cell in the center and a single surrounding layer of supporting cells (granulosa cells). After birth no new follicles are added to the reservoir and its size decays exponentially as individual follicles initiate growth and development. Follicle activation and growth is characterized by division of the granulosa cells to form additional layers that surround the egg. In humans the size of the immature reservoir is on the order of  $10^6$  follicles at birth and its half-life is approximately 10 years. Most developing follicles do not fully mature. After attaining different sizes the overwhelming majority of follicles (greater than 99% in humans) atrophy, that is, the cells within the follicle die and are removed, in a process called atresia. Eventually the entire follicle (including its egg) disappears from the ovary. The small number of developing follicles that do not become atretic but instead reach full maturity and release their egg during each ovulation cycle is the regulated ovulation number.

A hormonal mechanism for follicle interaction has been established. This interaction mechanism involves a feedback loop between ovarian follicles and the pituitary-hypothalamus. Removing the pituitary from an adult female results in the arrest of follicle growth. In such an animal, relatively immature follicles can be made to resume growth and ovulate by injecting extracts containing varying proportions of two purified pituitary gonadotropic hormones, FSH (follicle-stimulating hormone) and LH (luteinizing hormone). Maturation to ovulation can occur even when the nerve supply to the ovary is severed and it is transplanted to a different site in the organism.<sup>(3)</sup> Because a developing follicle secretes the hormone estradiol into the circulation at a rate that increases as it grows, follicle estradiol secretion rate can be used as a measure of follicle maturity. In 1981, Zeleznik showed that pituitary gonadotropin secretion is very sensitively inhibited by circulating estradiol concentrations at times when follicular development and the gradual emergence of ovulatory follicles are occurring.<sup>(4)</sup> This establishes a feedback mechanism where every estradiol-secreting follicle affects the maturation rate of every other such follicle (and

even itself) through its contribution to the circulating estradiol concentration and the effect that this hormone has on gonadotropin release. The following model shows that such interaction can account for the regulation of ovulation number.

## 2. MODEL FORMULATION

Let  $h_1(t)$  and  $h_2(t)$ , respectively, represent the concentrations of FSH and LH as functions of time in the circulation. We assume that these hormones are secreted into a blood volume  $V$  at rates  $\sigma_1$  and  $\sigma_2$  that depend upon the circulating concentration of estradiol  $X$ . If  $\gamma_1$  and  $\gamma_2$  are the first-order circulatory clearance constants for these hormones, then

$$V \frac{dh_1}{dt} = \sigma_1(X) - \gamma_1 h_1 \quad (1)$$

and

$$V \frac{dh_2}{dt} = \sigma_2(X) - \gamma_2 h_2 \quad (2)$$

If we measure the maturity of the  $i$ th follicle at time  $t$  by its estradiol secretion rate into the circulation  $s_i(t)$ , then we have a conservation equation for estradiol similar to (1) and (2),

$$V \frac{dX}{dt} = \sum_{j=1}^N s_j - \gamma_3 X \quad (3)$$

where the summation is over all  $N$  estradiol-secreting follicles and  $\gamma_3$  is the circulatory clearance constant for estradiol removal. Assuming that follicle maturation rate depends on both follicle maturity and the circulating concentrations of FSH and LH yields

$$\frac{ds_i}{dt} = \bar{g}_i(s_i, h_1, h_2) \quad (4)$$

In most mammalian species, follicle maturation occurs over a period of days to weeks. In comparison, the half-life of estradiol, FSH, and LH in the circulation and the response time of the pituitary–hypothalamic axis to circulating estradiol are short (a few minutes to an hour or two, depending on the species).<sup>(5–10)</sup> This means that the dynamics of (4) will be slow compared to (1)–(3) and therefore the solutions of (1)–(3) will always be near equilibrium on the time scale set by (4). If we make this quasiequilibrium

approximation for (1)–(3), then this produces the following simplified dynamical system:

$$\frac{dx_i}{dt} = g_i(x_i, X), \quad i = 1, \dots, N \quad (5)$$

$$X = \sum_{j=1}^N x_j \quad (6)$$

where

$$x_i(t) \equiv \frac{s_i(t)}{\gamma_3} \quad (7)$$

is the concentration that the  $i$ th follicle supports in the circulation at time  $t$ . Since  $x_i(t)$  is directly proportional to  $s_i(t)$ , it is an equivalent measure of follicle maturity. The system (5)–(6) is connected to (1)–(4) by (7) and

$$g_i(x_i, X) \equiv \bar{g}_i \left( \gamma_3 x_i, \frac{\sigma_1(X)}{\gamma_1}, \frac{\sigma_2(X)}{\gamma_2} \right) \quad (8)$$

Note that the effects of FSH and LH are still present in the system (5)–(6). Their effects are represented implicitly by (8).

The function  $g_i(x, X)$  in (5) determines the  $i$ th follicle's maturation rate for any given maturity  $x$  and circulating estradiol concentration  $X$ . Thus, any particular choice for  $g_i(x, X)$  in the model represents a possible program of follicle development. Since it is reasonable to assume that follicles in a given individual inherit a similar plan of growth, we will first consider the idealization where every model follicle of the system (5)–(6) inherits the same developmental program,

$$g_i(x, X) \equiv f(x, X) \quad \text{for all } i \quad (9)$$

Substituting (9) into (5) finally yields the form of the system we will analyze:

$$\frac{dx_i}{dt} = f(x_i, X), \quad i = 1, \dots, N \quad (10)$$

$$X = \sum_{j=1}^N x_j \quad (11)$$

In the system (10)–(11) the maturation of developing follicles is coupled through the variable  $X$ . This variable is a symmetric function (the sum function) of these maturities and this symmetry reflects the idea of inter-

action through circulatory feedback. Because  $f$  depends on  $x$  as well as  $X$ , model follicles with different maturities will, in general, develop at different rates even though every model follicle is assumed to have the *same* maturation program ( $f$ ) and at any instant receive the *same* circulating feedback signal  $X$ .

### 3. THEORY

We do not have a theory for analyzing the solutions to (10)–(11) for arbitrary  $f$  and initial conditions. It is possible, however, to analyze the qualitative behavior of the solutions to the initial value problem for a system of fixed but arbitrary size  $N$ , and for a limited class of interaction functions.<sup>(11–13)</sup> As a result of this analysis, we will demonstrate explicit follicle maturation functions that are capable of regulating ovulation number under more realistic physiological conditions where the number of developing follicles  $N$  in the interacting follicle population changes in time as new follicles initiate growth from a dormant reservoir and where  $f$  is similar but not identical for each interacting follicle.

We now consider the system (10)–(11) when  $x_i(0) = x_{i0}$ ,  $i = 1, \dots, N$ , and when  $f$  takes the form

$$\begin{aligned}
 f(x_i, X) &= x_i \phi(x_i, X) \\
 \phi(x_i, X) &= \delta(X) \left[ \rho(X) + \xi \left( \frac{x_i}{X} \right) \right]
 \end{aligned}
 \tag{12}$$

where  $\delta$  is any  $C^1$  positive-valued function and  $\rho$  and  $\xi$  are arbitrary  $C^1$  functions defined on appropriate physiological domains. For  $\delta$  and  $\rho$  this domain is  $X > 0$ , since negative concentrations have no physical meaning and the domain for  $\xi$  is  $[0, 1]$  because no follicle at any time  $t$  can support a circulating concentration  $x_i(t)$  greater than the total  $X(t)$ . Since  $f$  in (12) remains unchanged when any constant is subtracted from  $\xi$  and added to  $\rho$ , we will assume, without losing generality, that  $\xi(0) = 0$ . The function  $\phi$  can be interpreted as a relative growth rate. For a given value of  $X$

$$\tau_D(x, X) \equiv \frac{\ln 2}{\phi(x, X)}
 \tag{13}$$

represents the time it would take for a follicle with maturity  $x$  to double its estradiol secretion rate. If, for example, the estradiol secretion rate of a follicle were directly proportional to the number of estradiol-secreting (granulosa) cells it contained, then  $\phi$  would determine the doubling times of these cells as a function of follicle maturity (estradiol production rate)

and the circulating concentrations of FSH and LH (represented implicitly by  $X$ ).

Since  $\delta$  in (12) is assumed to be positive, a new time variable  $\tau$  can be defined by

$$\tau(t) \equiv \int_0^t \delta(X(s)) ds, \quad \text{or} \quad \frac{d\tau}{dt} = \delta(X(t)) \tag{14}$$

If we use this time scale and also scale follicle maturity so that it is a fraction between 0 and 1 by defining

$$y_i(\tau) \equiv \left[ \frac{x_i(t(\tau))}{X(t(\tau))} \right]^{1/2}, \quad i = 1, \dots, N \tag{15}$$

then the system (10)–(12) can be expressed in the following form:

$$\begin{aligned} \frac{dY}{d\tau} &= -\nabla_s V(Y) \\ V(Y) &= -\frac{1}{2} \sum_{i=1}^N \int_0^{y_i} s \xi(s^2) ds \\ S &= \left\{ Y: \sum_{i=1}^N y_i^2 = 1 \right\} \\ Y(0) &= Y_0 \in S \end{aligned} \tag{16}$$

where  $Y = (y_1, \dots, y_N)$ .

The dynamical system (16) is a gradient system on the unit sphere  $S$  in  $\mathfrak{R}^N$  and therefore can be given a rather simple geometric interpretation. Any solution curve  $Y(\tau)$  of the system can be viewed as being generated by a point moving on  $S$  with velocity  $dY/d\tau$ . If  $V(Y)$  defines the height above the surface  $S$  at  $Y$ , then  $V$  generates a relief map on the sphere  $S$ . Note that  $V$  depends only on  $\xi$  and not on the  $\delta$  or  $\rho$  functions. At any point  $Y$  on  $S$ ,  $-dY/d\tau$  is the gradient of  $V$  on  $S$  ( $\nabla_s V$ ). More precisely,

$$\nabla_s V = \nabla V - \langle \nabla V, Y \rangle Y \tag{17}$$

which says that  $\nabla_s V$  can be calculated from the gradient of  $V$ , by projecting it onto the tangent plane of  $S$  at  $Y$ . (Since the domain of  $\xi$  is the unit interval  $[0, 1]$ , the domain of  $V$  is the unit cube in  $\mathfrak{R}^N$ .) Let  $\bar{V}$  define  $V$  as a function of  $\tau$  along a solution curve  $Y(\tau)$ . Then,

$$\frac{d\bar{V}}{d\tau} = \frac{dV(Y(\tau))}{dt} = \left\langle \nabla V(Y), \frac{dY}{dt} \right\rangle = -\|\nabla_s V(Y)\|^2 \leq 0 \tag{18}$$

which implies that  $\bar{V}$  is strictly decreasing for nonequilibrium solutions. Limiting values of  $\bar{V}$  occur at equilibria of the system. Geometrically these correspond to those points  $Y_e$  that are critical values of  $V$  on  $S$ . In general, when there is a finite number of equilibria and these are nondegenerate (zero is not an eigenvalue of the linearization) then every solution curve of a gradient system will approach an equilibrium as  $\tau \rightarrow \infty$ . Therefore, a solution cannot be a closed curve or a path that continually wanders in some manifold of  $S$ : all solutions dissipate asymptotically in time to an equilibrium. Since (18) shows that all nonequilibrium solutions move “downhill,” stable equilibria of the system will correspond to relative minima of  $V$  on  $S$  where no local path of further descent exists.

The components of critical points  $Y_e$  of  $V$  on  $S$  satisfy

$$-\frac{1}{2} y_i \left[ \xi(y_i^2) - \sum_{j=1}^N y_j^2 \xi(y_j^2) \right] = 0, \quad i = 1, \dots, N \tag{19}$$

Therefore the equilibria  $Y_e$  of the system (16) can be described in the following way. An equilibrium with  $M$  nonzero coordinates will be called an  $M$ -fold equilibrium. The point

$$Y_e = (\underbrace{a_1, a_2, \dots, a_M}_M, \underbrace{0, \dots, 0}_{N-M}) \tag{20}$$

is an  $M$ -fold equilibrium if the  $a_i \neq 0, i = 1, \dots, M$ ,

$$\sum_{i=1}^M a_i^2 = 1 \tag{21}$$

and  $\xi$  maps every  $a_i^2$  to a common value, that is, if

$$\lambda(Y_e) \equiv \xi(a_i^2) \quad \text{for all } i = 1, \dots, M \tag{22}$$

An easy way to satisfy (22) is to make all the  $a_i$  equal. This yields equilibria of the form

$$Y_e = (\underbrace{1/\sqrt{M}, 1/\sqrt{M}, \dots, 1/\sqrt{M}}_M, \underbrace{0, \dots, 0}_{N-M}), \quad M = 1, \dots, N \tag{23}$$

where  $\lambda = \xi(1/M)$ . These equilibria are denoted as  $M$ -fold symmetric. Note that any permutation of the  $N$  coordinates of an  $M$ -fold equilibrium is also an  $M$ -fold equilibrium. Solving for those critical points that correspond to local minima of  $V$  on  $S$  leads to the following stability theorem.<sup>(11)</sup>

**Theorem 3.1.** An  $M$ -fold nondegenerate equilibrium  $Y_e$  is stable (a local minimum of  $V$  on  $S$ ) if and only if the common value  $\lambda = \xi(a_i^2) > 0$  for

all coordinates  $a_i \neq 0$  and either the derivative  $\xi'(a_i^2) < 0$  for all of the non-zero coordinates or  $\xi'(a_i^2) \geq 0$  for exactly one nonzero coordinate and

$$\sum_{i=1}^M [\xi'(a_i^2)]^{-1} > 0 \quad (24)$$

(by convention  $1/0 = +\infty$ ).

The set of points of  $S$  that approach unstable equilibria comprise a set of measure zero. Finding the set of physically relevant eventual maturational states of the system of  $N$  interacting follicles satisfying (10)–(12) is therefore equivalent to applying Theorem 3.1 to locate the stable equilibria of (16) and interpreting these stable equilibria in terms of the original coordinate system. In the next section we will demonstrate this procedure for a simple example.

#### 4. AN EXAMPLE

Consider a system of  $N$  interacting follicles that obey (10)–(11) where the follicle interaction function takes the form

$$f(x, X) = x\phi(x, X) = x\{K - D(X - M_1x)(X - M_2x)\} \quad (25)$$

$$\frac{1}{M_1} + \frac{1}{M_2} < 1 \quad (25a)$$

The parameters  $K$  [time<sup>-1</sup>],  $D$  [concentration<sup>-2</sup> time<sup>-1</sup>],  $M_1$ , and  $M_2$  are positive, real valued, and are the same for all  $N$  interacting follicles. Although  $K$  and  $D$  can be scaled to 1 by choosing appropriate units for concentration and time,  $M_1$  and  $M_2$  are dimensionless. The quadratic polynomial for the relative growth rate function  $\phi$  in (25) is believed to be the simplest and lowest-degree polynomial that can regulate ovulation number within a finite adjustable interval of integers. It has the following physiological features:

1. When the circulating estradiol concentration  $X$  is sufficiently small (this also implies that follicle maturity  $x$  will be sufficiently small), follicles will grow independently and exponentially with rate constant  $K$ .
2. For any fixed value of  $X$ , there exists an interval of follicle maturities where the growth rate  $f$  is positive. Outside this "window" of growth, follicles undergo atresia (negative growth).
3. As  $X$  increases (FSH decreases), this window of growth moves toward higher maturities, and the minimum follicle maturity required to escape atresia increases.

Although experimental techniques have not yet been developed to determine explicitly the form of  $f$  in any mammal, the physiological features described above are consistent with experimental observations.<sup>(14-16)</sup> These physiological properties were not explicitly used, however, to construct the follicle interaction function (25). They are consequences of the construction method described below.

The function (25) can be written in the form of (12) where

$$\delta(X) = X^2, \tag{26}$$

$$\rho(X) = \frac{K}{X^2} - D \tag{27}$$

$$\xi(p) = Dp(M_1 + M_2 - M_1M_2p), \quad p = \frac{x}{X} \tag{28}$$

The function  $\xi$  is a parabola with roots at 0 and  $p^* = 2/M_H$  (Fig. 1). The maximum occurs at  $p^{**} = 1/M_H$ , where the value  $M_H$  is the harmonic mean of  $M_1$  and  $M_2$ ,

$$\frac{1}{M_H} = \frac{1}{2} \left( \frac{1}{M_1} + \frac{1}{M_2} \right) \tag{29}$$

Theorem 3.1 says that a symmetric  $M$ -fold equilibrium will be stable if  $\xi(1/M) > 0$  and  $\xi'(1/M) < 0$ . Figure 1 shows that this occurs for all values

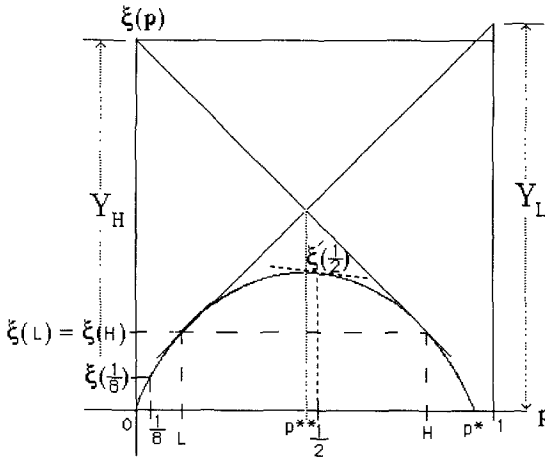


Fig. 1. An example of a graph of  $\xi$  vs.  $p$  from an  $f$  that satisfies (25)–(25a) and regulates ovulation number at 2. The only stable equilibria are the 2-fold symmetric, because  $M = 2$  is the only integer value that satisfies  $\xi(1/M) > 0$  and  $\xi'(1/M) < 0$ . All nonsymmetric equilibria are unstable since  $p^{**} < 1/2$  and therefore  $Y_H < Y_L$  for all possible values of  $\xi(p)$ .

of  $1/M$  that lie in the interval  $(p^{**}, p^*)$ . Therefore stable  $M$ -fold symmetric equilibria occur for those values of  $M$  that satisfy

$$\frac{1}{2}M_H < M < M_H \tag{30}$$

The graphical method described above can be generalized and applied to any  $C^1$  function  $\xi$  on  $[0, 1]$  with  $\xi(0)=0$ . Stable  $M$ -fold symmetric equilibria will occur for those values of  $1/M$  that lie in intervals where both the graph  $\xi$  lies above the  $x$  axis and where  $\xi$  has a negative slope.

When the graph of  $\xi$  is concave down and has a single maximum in the interior of  $[0, 1]$ , then a graphical method can also be used to determine the stability of nonsymmetric equilibria. Consider a line parallel to the  $x$  axis that intersects the graph of  $\xi(p)$  at two points (Fig. 1). Let  $(L, \xi(L))$  be the left intersection and  $(H, \xi(H))$  be the right. According to Theorem 3.1, any stable, nonsymmetric  $M$ -fold equilibrium must have coordinates

$$Y_e = (\underbrace{\sqrt{L}, \sqrt{H}, \dots, \sqrt{H}}_{M}, \underbrace{0, \dots, 0}_{N-M}) \tag{31}$$

or permutations of these coordinates. In addition, since  $Y_e$  must be on  $S$  and satisfy (24), there are two additional constraints. These are

$$L + H(M - 1) = 1 \tag{32}$$

and

$$\frac{1}{\xi'(L)} + \frac{M-1}{\xi'(H)} > 0 \tag{33}$$

Using (32) to eliminate  $M - 1$  from (33) yields

$$(1 - L) \xi'(L) < -H\xi'(H) \tag{33a}$$

This result has a geometric interpretation (Fig. 1). The tangent line at  $(H, \xi(H))$  intersects the  $y$  axis at  $Y_H = -H\xi'(H) + \lambda$  and the tangent line at  $(L, \xi(L))$  intersects the vertical line  $p=1$  at  $Y_L = (1 - L)\xi'(L) + \lambda$ , where  $\lambda = \xi(L) = \xi(H)$ . Therefore, (31) will be unstable if  $Y_H < Y_L$ . The symmetry of parabolic functions defined by (28) requires that the two tangent lines intersect with equal and opposite slope at  $p^{**} = 1/M_H$  and therefore stable nonsymmetric equilibria will not exist if  $p^{**} < 1/2$ , i.e.,  $M_H > 2$ . This is ensured by (25a). Therefore, for the class of follicle interaction functions represented by (25)–(25a), every initial state on the unit

sphere, except for a set of measure zero, flows asymptotically to an  $M$ -fold symmetric equilibrium with  $M$  an integer in the interval  $(M_H/2, M_H)$ . This class of follicle interaction functions therefore carves the sphere into a finite number of open set regions (valleys of  $V$ ), where each region  $R_M$  is assigned an integer in the interval  $(M_H/2, M_H)$  corresponding to the stable  $M$ -fold symmetric equilibrium that all points in the region approach as  $\tau \rightarrow \infty$ . The boundaries of these regions are comprised of the unstable equilibria and the set of points that flow into them.

To interpret these results physically, it is necessary to return to the original coordinate system. The circulating estradiol concentration expressed as a function of  $\tau$  satisfies

$$\frac{d\bar{X}}{d\tau} = \bar{X} \left[ \rho(\bar{X}) + \sum_{i=1}^N y_i^2 \xi(y_i^2) \right] \quad (34)$$

where  $\bar{X}(\tau) = X(t(\tau))$ . Consider the set of initial points  $R_M$  on  $S$  that flow into the  $M$ -fold stable symmetric equilibrium. For these points

$$\sum_{i=1}^N y_j^2 \xi(y_j^2) \rightarrow \lambda(Y_e) = \xi\left(\frac{1}{M}\right) \quad \text{as } \tau \rightarrow \infty \quad (35)$$

and therefore after a sufficiently long time

$$\frac{d\bar{X}}{d\tau} \approx \bar{X} \left[ \rho(\bar{X}) + \xi\left(\frac{1}{M}\right) \right] \quad (36)$$

For the follicle interaction function (25),  $\rho$  is the decreasing function (27) with  $\inf \rho = -D$ . We now consider two possible cases, depending on whether  $\xi(1/M) < D$  or  $\xi(1/M) > D$  for  $M \in (\frac{1}{2}M_H, M_H)$ . These cases represent idealizations of two types of reproductive strategies that are observed in higher mammals—induced and spontaneous ovulators.

For induced ovulators (rabbits are an example), the process regulating follicle maturation is distinct from the mechanism that actually triggers ovulation, that is, the release of eggs from mature follicles into the oviducts (fallopian tubes). A number of follicles in a well-controlled range reach ovulatory maturity at a time when the circulating estradiol concentration has reached a relatively steady level. This level is sufficiently high to make the female responsive to male advances, but insufficient by itself to spontaneously cause ovulation. The separate event of intercourse must occur to induce ovulation of the mature follicles. Nerve endings in the vagina are activated by the mechanical stimulation of intercourse and produce a surge of gonadotropin from the pituitary-hypothalamus. This surge and the

subsequent ovulation event occur on a time scale that is usually short in comparison to the follicle maturation process.

In the case of the spontaneous ovulator (humans are an example), the estradiol concentrations never reach steady levels, but continue to rise at increasing rates until a concentration and/or rate is attained that spontaneously triggers the gonadotropic surge and ovulation of a well-controlled number of mature follicles. This happens if intercourse has occurred or not. As in the case of the induced ovulator, the gonadotropic surge mechanism and subsequent ovulation event occur on a relatively short time scale compared to the mechanism that regulates follicle maturation. In both spontaneous and induced ovulators, the hypothalamic location of the gonadotropic surge mechanism is believed to be anatomically distinct from the estradiol-gonadotropin feedback mechanism regulating follicle maturation. It is this latter maturation process and not the gonadotropic surge mechanism that is being modeled here.

**Case 1. Induced Ovulator:  $\xi(1/M) < D$  for  $M \in (\frac{1}{2}M_H, M_H)$**

For each  $M$ , there is a unique root  $\bar{X} = X_\infty(M)$  of  $\rho(\bar{X}) + \xi(1/M)$ . This root is a stable equilibrium of (36) and therefore also of (34). Thus,  $\lim_{\tau \rightarrow \infty} \bar{X} = X_\infty(M)$  for all initial states,  $Y_0 \in R_M$ . Using (14), we have

$$\frac{dt}{d\tau} = \frac{1}{\delta(\bar{X})} \approx \frac{1}{\delta(X_\infty)} > 0 \tag{37}$$

This means that  $\lim_{\tau \rightarrow \infty} t = \infty$  and therefore  $\lim_{t \rightarrow \infty} X = X_\infty(M)$ . From the definition (15) of  $y_i$ , the estradiol concentration that the  $i$ th follicle supports at time  $t$  is

$$x_i(t) = y_i^2(\tau(t)) X(t), \quad i = 1, \dots, N \tag{38}$$

For each point in  $R_M$ ,  $M$  coordinates will satisfy  $y_i \rightarrow 1/\sqrt{M}$  as  $\tau \rightarrow \infty$  and the remaining  $N - M$  coordinates will satisfy  $y_i \rightarrow 0$  as  $\tau \rightarrow \infty$ . Therefore,

$$\text{if } \lim_{\tau \rightarrow \infty} y_i = \begin{cases} \frac{1}{\sqrt{M}}, \\ 0, \end{cases} \quad \begin{array}{l} \text{then } \lim_{t \rightarrow \infty} x_i = \frac{X_\infty(M)}{M} \\ \text{then } \lim_{t \rightarrow \infty} x_i = 0 \end{array} \tag{39}$$

That is,  $M$  follicles will emerge from the follicle population with the same equilibrium maturity, while the remainder will undergo atresia. The ovulation number  $M$  will depend on the initial state of the system; however, it will always be an integer in the interval  $(M_H/2, M_H)$  independent of the

size  $N$  of the system. Of course, intercourse or some other mechanism will eventually cause follicle turnover from the equilibrium pool of mature follicles before  $\tau \rightarrow \infty$ .

**Case 2. Spontaneous Ovulator:  $\xi(1/M) > D$  for  $M \in (\frac{1}{2}M_H, M_H)$**

Since  $\rho(\bar{X}) > -D$  for all  $\bar{X}$ , after sufficiently large  $\tau$ ,

$$\frac{d\bar{X}}{d\tau} > K\bar{X} \tag{40}$$

where  $K = \xi(1/M) - D > 0$ . This implies

$$\lim_{\tau \rightarrow \infty} \bar{X} = \infty \tag{41}$$

What happens to the time  $t$  as  $\tau \rightarrow \infty$ ? Using (14) to solve for  $t(\tau)$  yields

$$t(\tau) = \int_0^\infty \frac{d\tau}{\delta(\bar{X})} = \int_{\bar{X}(0)}^{\bar{X}(\infty)} \frac{1}{\delta(\bar{X})} \frac{d\tau}{d\bar{X}} d\bar{X} \tag{42}$$

For  $\tau > \tau_1$ , where  $\tau_1$  is a sufficiently large number, we can use (40) to obtain

$$\lim_{\tau \rightarrow \infty} t(\tau) < \int_0^{\tau_1} \frac{d\tau}{\delta(\bar{X})} + \frac{1}{K} \int_{\bar{X}(\tau_1)}^\infty \frac{d\bar{X}}{\bar{X} \delta(\bar{X})} \tag{43}$$

The right-hand side of (43) will be bounded as  $\tau \rightarrow \infty$  if  $\delta(X)$  grows faster than  $X^\epsilon$  as  $X \rightarrow \infty$ , where  $\epsilon > 0$ . This condition is satisfied for the follicle interaction function (25), which has a  $\delta$  given by (26). Therefore,

$$\lim_{\tau \rightarrow \infty} t = T(Y_0) \tag{44}$$

where  $T$  is a finite time that depends on the initial state  $Y_0 \in R_M$ . Combining (41) and (44), we have  $\lim_{t \rightarrow T(Y_0)} X(t; Y_0) = \infty$ . Applying this result to (38) shows that if  $\lim_{\tau \rightarrow \infty} y_i = 1/\sqrt{M}$ , then for the follicles that correspond to these coordinates  $\lim_{t \rightarrow T} x_i = \infty$ .

When expressed as a function of  $\tau$ , follicle maturity satisfies

$$\frac{d\bar{x}_i}{d\tau} = \bar{x}_i [\rho(\bar{X}) + \xi(y_i^2)] \tag{45}$$

where  $\bar{x}_i(\tau) = x_i(t(\tau))$ . If  $y_i \rightarrow 0$  as  $\tau \rightarrow \infty$ , then  $\xi(y_i^2) \rightarrow 0$ . Thus, for the follicles that correspond to these coordinates, we have

$$\frac{d\bar{x}_i}{d\tau} \approx -D\bar{x}_i \tag{46}$$

since  $\rho(\bar{X}) \rightarrow -D$  for sufficiently large  $\tau$ . Therefore, for these follicles  $x_i \rightarrow 0$  as  $t \rightarrow T$ . In summary, for every initial state of the  $N$ -follicle system that corresponds to a point  $Y_0 \in R_M$ ,  $M$  follicles will emerge with unbounded maturity in a finite time, while the remaining follicles will undergo atresia. The ratio of maturities of any two follicles that do not become atretic approaches unity as  $t \rightarrow T$ . Of course, neither follicle maturity nor the circulating estradiol concentration can physically grow without bound. Eventually  $X$  and/or  $dX/dt$  will become sufficiently large to signal the gonadotropic surge mechanism that signals ovulation. At this time  $M$  follicles will have been selected with ovulation maturities whose ratios approach unity. A finite "blowup" time  $T(Y_0)$  is an idealization that allows the model to make predictions about ovulation time as well as ovulation number for the spontaneous ovulator.

As in the case of the induced ovulator, the ovulation number  $M$  is limited to be within the range  $(M_H/2, M_H)$  and this interval is independent of  $N$ . This latter fact can account for the observation that the range of ovulation numbers for any given mammal is largely insensitive to the surgical removal of ovarian tissue or to the age of the mammal.

## 5. SOME NUMERICAL EXAMPLES

In this section we illustrate some of the theoretical results obtained in the previous section with numerical examples. We will also simulate the behavior of the system under physiological conditions that cannot be fully analyzed by the methods introduced in the previous section.

Figure 2 shows the graphical results of four typical numerical solutions of the system (10)–(11) with  $f$  as in (25)–(25a). The initial maturity of each follicle is chosen independently from a uniform distribution and the parameters for  $M_1$  and  $M_2$  are chosen so that only the integer value  $M = 2$  is in the stable interval  $(M_H/2, M_H)$ . Since the value of  $D > \xi(1/2)$ , two follicles emerge from the population with the same equilibrium maturity, while the remainder atrophy. This example models an induced ovulator that regulates ovulation number at *two* independent of the number of interacting follicles or their initial maturities. The equilibrium (ovulatory) maturity is also independent of the size of the follicle population and its initial state. Note that it is always the two initially largest follicles that emerge as ovulatory. In fact, it can be proven that the initial order of follicle maturities must be maintained. However, if we allow the parameters of  $f$  to vary somewhat among follicles, then crossovers in follicle maturity can occur. This is shown in Fig. 3, where the growth function parameters for each follicle are chosen independently from a uniform distribution. In

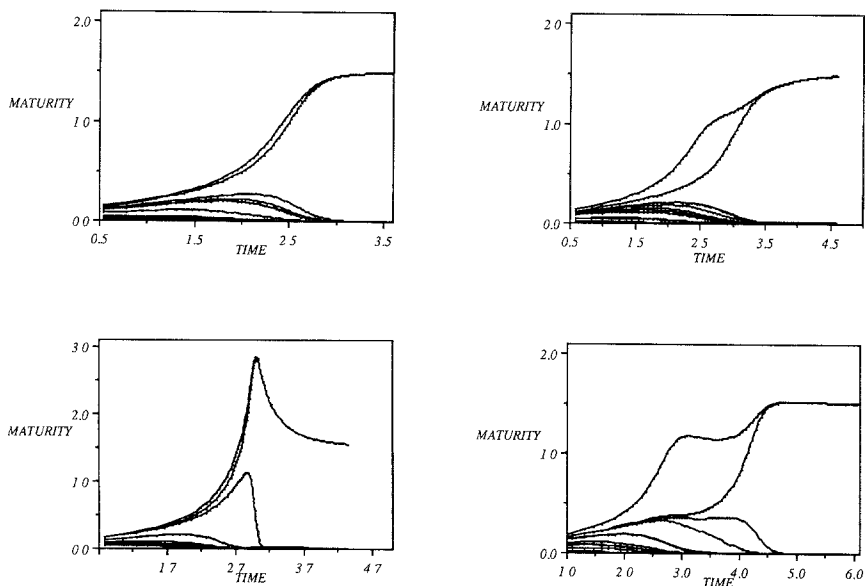


Fig. 2. The graphs of four numerical solutions for the system (10)–(11) with  $f$  as in (25)–(25a). The parameters of  $f$  are  $M_1 = 2.2$ ,  $M_2 = 4.2$ ,  $D = 1.0$ ,  $K = 1.0$ .  $M_H$ , the harmonic mean of  $M_1$  and  $M_2$ , is 2.88, and therefore the stable interval  $(M_H/2, M_H)$  contains only one integer,  $M = 2$ . The number of follicles in each graph is  $N = 10$ . Initial follicle maturities are chosen independently from a uniform distribution in the interval  $[0, 0.1]$ . Two follicles approach the same equilibrium maturity independent of the initial conditions, while the remainder atrophy. This models an induced ovulator that regulates ovulation number at 2.

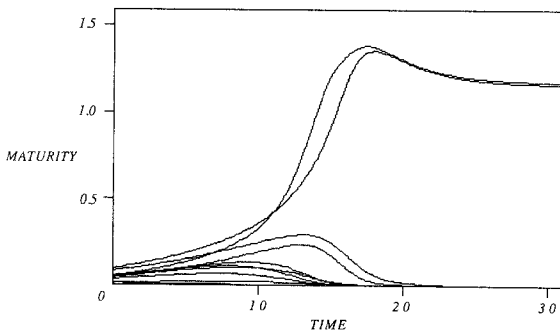


Fig. 3. The graph of a numerical solution to the system (5)–(6) showing follicle maturation curves that cross each other. The number of interacting follicles is  $N = 10$ . Each follicle satisfies a growth function  $(g_i(x, X))$  of the form (25), but the values of the parameters of  $f$  for each follicle are chosen independently from uniform distributions. The intervals for these distributions are:  $2.2 < M_1 < 2.42$ ,  $4.2 < M_2 < 5.04$ ,  $1.03 < D < 2.06$ ,  $1.07 < K < 2.14$ . Initial follicle maturities are also chosen from a uniform distribution in the interval  $[0, 0.1]$ .

this case the numerical solutions pertain to a system of the more general form (5)–(6) rather than (10)–(11).

Figure 4 illustrates two numerical solutions of (10)–(11) with  $f$  as in (25)–(25a). In this case the parameters of  $f$  have been chosen so that there are several integers in the stable range ( $M_H/2 = 3.02$ ,  $M_H = 6.04$ ). Ovulation number now depends on the initial state of the system, but will always be 4, 5, or 6 independent of size of the interacting follicle population. Since  $D < \xi(1/M)$  for  $M = 4, 5, 6$ , this example corresponds to the spontaneous

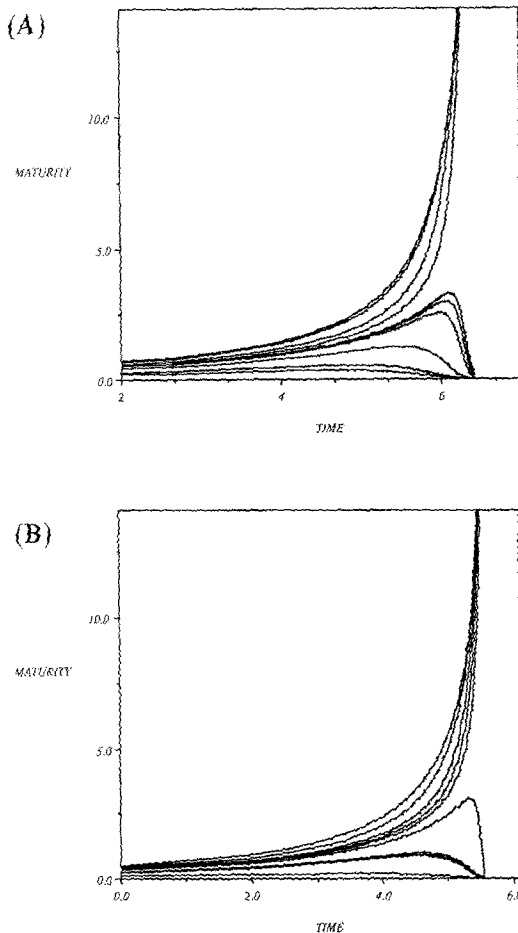


Fig. 4. The graphs of two numerical solutions of the system (10)–(11) with  $f$  as in (25),  $M_1 = 3.95$ ,  $M_2 = 12.9$ ,  $D = 0.004$ ,  $K = 4.0$ . Since  $M_H = 6.048$ , the stable range of integers is [4, 6]. This example corresponds to a spontaneous ovulator because  $\xi(1/4)$ ,  $\xi(1/5)$ ,  $\xi(1/6)$  are all larger than  $D$ . (A) Four follicles ovulate, (B) the ovulation number is 5.

ovulator of Section 5 (Case 2) in which both ovulation number and ovulation time are predicted by the model. The ovulation (“blowup”) time depends on the initial conditions.

It is natural to consider the behavior of this hormonal feedback system when  $N$ , the number of interacting follicles, is not fixed, but changes in time as new follicles initiate growth from a dormant immature pool. This motivates a model of the following form:

$$\begin{aligned} & \{t_i: i = 1, 2, \dots\} \\ x_i &= \begin{cases} 0 & t < t_i \\ x_i^* & t = t_i \end{cases} \\ & i = 1, 2, \dots \end{aligned} \tag{47}$$

$$\frac{dx_i}{dt} = g_i(x_i, X), \quad t \geq t_i$$

$$X(t) = \sum_i x_i(t)$$

where  $t_i$  denotes the activation time of the  $i$ th follicle. When  $t < t_i$  the  $i$ th follicle is dormant ( $x_i = 0$ ). At  $t = t_i$  it is activated with initial maturity  $x_i^*$  and for all times thereafter it satisfies the differential equation in (47) with the coupling global feedback variable  $X(t)$  defined again as the total estradiol concentration in the circulation at time  $t$ . Figure 5 displays a numerical solution of (47) when the activation times are chosen inde-

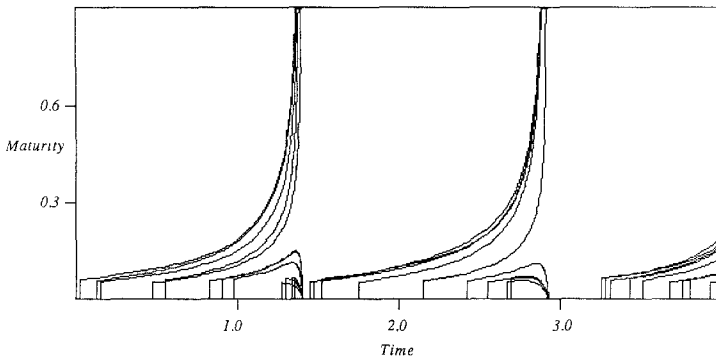


Fig. 5. Numerical solutions to the system (47) with random follicle entry. Activation times are chosen from a Poisson process with mean activation rate  $\mu = 8$ . Parameter values for the growth function of each follicle are selected from uniform distributions on the following intervals:  $3.6 < M_1 < 3.96$ ,  $22.32 < M_2 < 24.55$ ,  $1.03 < D < 1.133$ ,  $1.07 < K < 1.284$ .  $x_i^*$  is selected from a uniform distribution in the interval  $[0.3, 0.039]$ . Here  $X^\dagger = 20$ .

pendently from a Poisson process. The follicle growth functions are of the form (25),

$$g_i(x, X) = x \{ K_i - D_i (X - M_{1i} x) (X - M_{2i} x) \} \quad (48)$$

with parameter values that are selected independently from a uniform distribution. The  $x_i^*$  are also independently given values from a uniform distribution. The system self-organizes in time and "cycles" of maturation develop in which the ovulation number and time are well controlled. When the estradiol concentration reaches a critical value  $X = X^\dagger$  the follicles that have emerged as ovulatory are removed from the interacting population. This corresponds to the actual event of ovulation that is stimulated by estradiol through its activation of the gonadotropin surge mechanism (see Section 4). Histograms of the results of 1000 cycles are shown in Figs. 6 and 7. Using the theoretical results of Section 4 and the mean values of the parameters, it is possible to predict the correct ovulation numbers illustrated in Fig. 6; however, the analysis is significantly complicated by the presence of follicle entry at random times. New phenomena arise in this setting, including the existence of new equilibria and changes in stability of the symmetric equilibria.<sup>(17)</sup> The unimodal character of the ovulation time distribution and the fact that it is skewed right are typical of the distribution of ovulation times observed in spontaneous ovulators such as humans (Fig. 7).

The effects of removing an ovary in the middle of a cycle are simulated in Fig. 8. Follicles are randomly assigned left or right. At the time indicated by the arrow in Fig. 8, all follicles assigned to the right ovary are

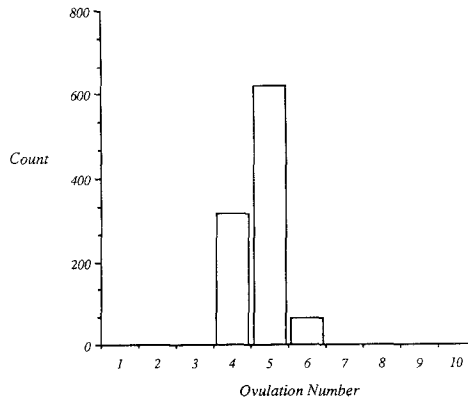
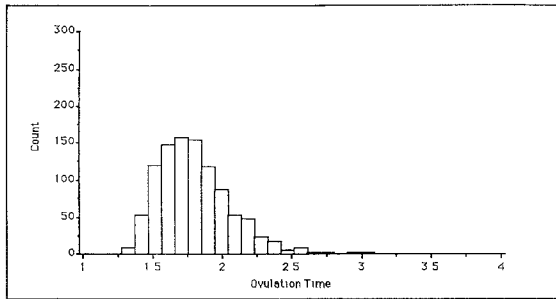
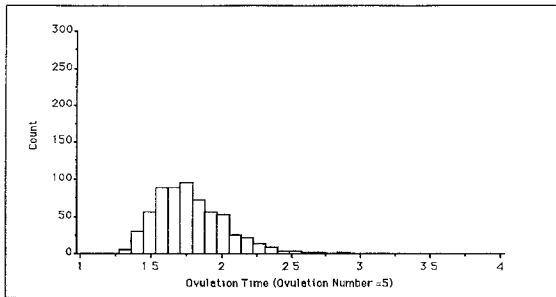


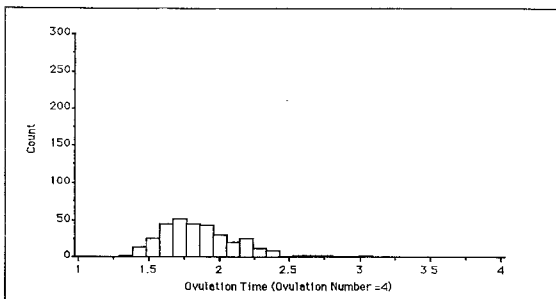
Fig. 6. A histogram of the ovulation numbers obtained in 1000 cycles with parameters as described in Fig. 5. Statistics: Mean = 4.747, standard deviation = 0.562.



(A)



(B)



(C)

Fig. 7. (A) Histogram of the ovulation time  $T$  defined by  $X(T) = X^{\dagger}$  for the 1000 cycles described in Figs. 5 and 6. Mean = 1.796, SD = 0.253. (B) Histogram of a subset of the 1000 cycles that correspond to those times in which the ovulation number = 5, mean = 1.783, SD = 0.244. (C) Histogram of a subset of the 1000 cycles that correspond to those times in which the ovulation number = 4, mean = 1.853, SD = 0.262.

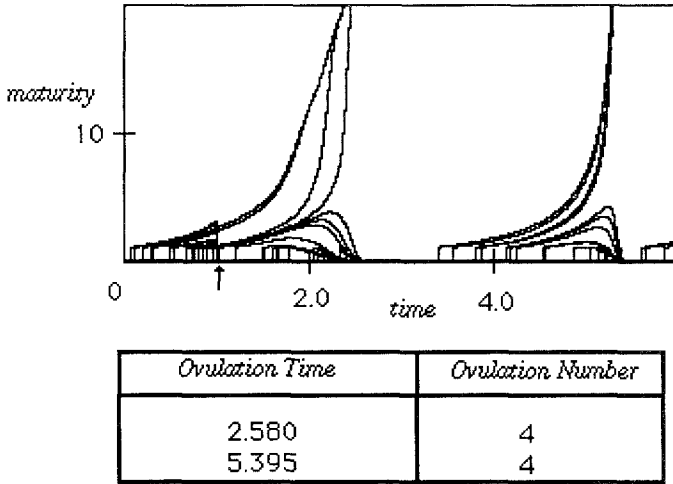


Fig. 8. Simulation of ovary removal in the middle of a cycle. The system satisfies (47) with  $g$ , satisfying  $f$  as in (25) with parameter values  $M_1 = 3.85$ ,  $M_2 = 15.15$ ,  $D = 0.0025$ ,  $K = 1.0$ . Follicles are activated by a Poisson process with mean rate  $\mu = 12$ . Here  $x_t^* = 2$  and  $X^\dagger = 20$ . Half of the follicles chosen at random are removed at  $t = 1$  (arrow). Ovulation number is conserved at 4.

eliminated from (47). In this case two of the largest follicles are removed. Nevertheless, the system automatically compensates for their elimination and ovulates the same number as if two ovaries were present (Lipschütz's law of follicular constancy (see Introduction)).<sup>(1,2)</sup>

Although the stable range of ovulation numbers is unaffected by the size of the interacting follicle population, there are subtle changes in the probability of observing a given ovulation number with  $N$ . This is illustrated in the histograms of Fig. 9. It is biological fact that the number of follicles interacting in each cycle slowly decreases with age as the size of the reserve follicle pool declines. In most mammals death ensues before the reserve pool of immature follicles is greatly exhausted; however, in humans complete or nearly complete exhaustion is the rule and marks the initiation of the menopausal period. In the human population the observed frequency of dizygotic twins (double ovulations) increases steadily with age until menopause is reached. (The monozygotic twin rate is unaffected by age.) An increase in the frequency of double ovulations in the human population with decreasing  $N$  is consistent with the results of the simulation in Fig. 9. As  $N$  decreases, the probability of observing a larger ovulation number in the allowable range increases, that is, the ovulation-number histograms shift to the right with decreasing  $N$ . There is a loss in the regulation of ovulation time as  $N$  decreases which is also consistent with observed

results: the dispersion of ovulation times increases as menopause is approached.

These results suggest an important physiological role for the large number of follicles that undergo atresia in all mammals. Most forms of plant and animal life have reproductive systems that are designed to release

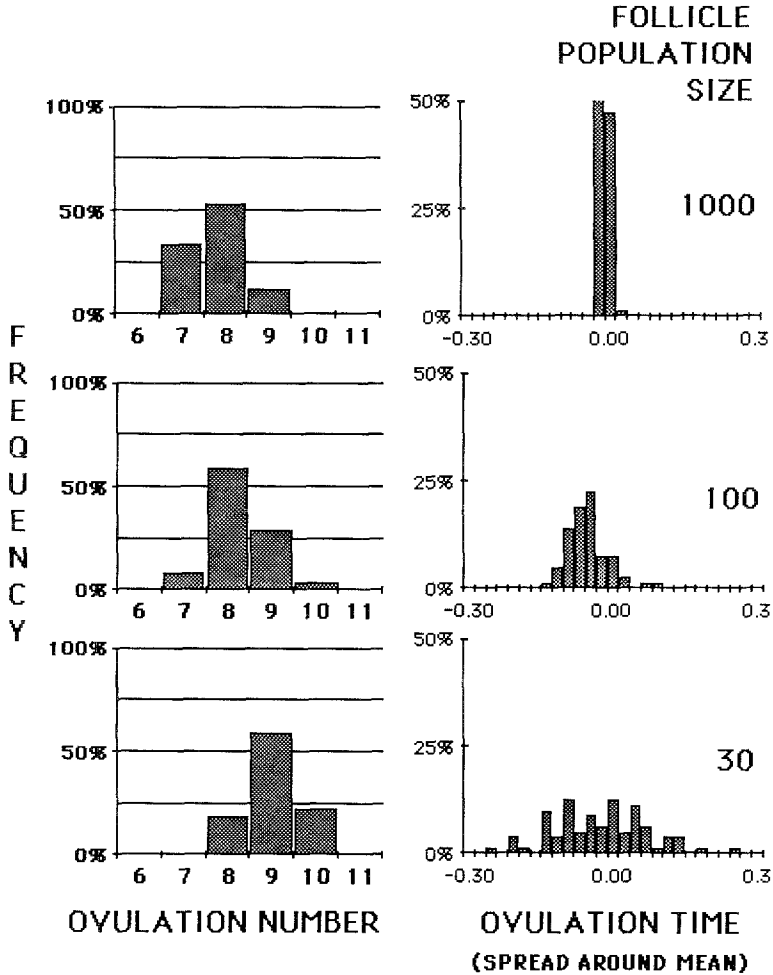


Fig. 9. The effect of the number of interacting follicles,  $N$ , on the regulation of ovulation number and time. Top:  $N=1000$ , ovulation number =  $7.79 \pm 0.65$  (mean  $\pm$  SD), ovulation time =  $4.37 \pm 0.01$ . Middle:  $N=100$ , ovulation number =  $8.28 \pm 0.67$ , ovulation time =  $5.55 \pm 0.04$ . Bottom:  $N=30$ , ovulation number =  $9.04 \pm 0.65$ , ovulation time =  $6.33 \pm 0.1$ . Each graph is the result of 80 numerical solutions of the initial value problem (10)–(11) with  $f$  as in (25)–(25a).  $M_1=6.1$ ,  $M_2=5000.0$ ,  $D=1.0$ ,  $K=1.0$ . Initial maturites are chosen independently from a uniform distribution in the interval  $[0, 10^{-5}]$ .

large numbers of eggs ( $10^5$ – $10^7$ ) into the external environment at times that are propitious for subsequent fertilization and development. This reproductive strategy has been altered in the warm-blooded vertebrates (mammals and birds), where only a few ( $10^0$ – $10^1$ ) eggs are released and develop within the spatially confined but well-regulated environment of the nest or uterus. The model suggests that in warm-blooded vertebrates, the older evolutionary scheme that activates a large number of follicles has not been discarded. Instead, this scheme has been adapted by a superimposed hormonal feedback mechanism to the (opposite) purpose of keeping the ovulation number down. It is not unusual in biology for older control mechanisms to be adapted rather than discarded as new control systems develop in response to changing environmental demands. In this case, it can be argued that the activation of a large number of follicles also helps the hormonal feedback system to better control the timing of ovulation. It appears that the distribution of ovulation times approaches a delta function as  $N \rightarrow \infty$ . This is also an interesting mathematical result because the distribution of ovulation numbers does not collapse on a single ovulation number as  $N \rightarrow \infty$ , but seems to approach a definite limiting form. Since each ovulation number has its own distribution of ovulation times (Fig. 7), it would not have been surprising, for example, if instead of a single peak, the distribution of ovulation times had several peaks—one for each ovulation number.

## 6. EXPERIMENTAL SUPPORT FOR THE ASSUMPTION OF NONSPATIAL FOLLICLE INTERACTION

For nearly a century there has accumulated a great deal of biological evidence to support the assumption that hormonal feedback plays a significant role in the regulation of follicle growth. We have shown here that this interaction can account for the regulation of ovulation number and several other biological features associated with it. What is the evidence, however, that spatially *dependent* interactions are not also significant in regulating follicle growth and ovulation number? It has been observed in several multiple ovulating mammalian species that the number of eggs released at the time of ovulation is distributed binomially between the left and right ovaries.<sup>(18-23)</sup> More precisely, if  $M$  is the total number of eggs released at the time of ovulation and if  $p_0$  is the probability that an egg is shed from the right (left) side, then the probability that  $k = 0, 1, \dots, M$  follicles reach ovulation maturity on the right (left) side satisfies

$$P(k) = \frac{M!}{k! (M - k)!} p_0^k (1 - p_0)^{M - k} \quad (49)$$

In those species studied  $p_0$  is close to  $1/2$ . The binomial result is, of course, consistent with a spatially independent feedback mechanism, but it is not, in general, consistent with a significant role for spatially dependent follicle–follicle interaction. Suppose that in addition to hormonal feedback, follicles secrete chemicals in proportion to their size and suppose that these chemicals stimulate (inhibit) the growth of neighboring follicles. Under these conditions the more extreme (central) values of  $k$  would be favored over expected binomial probabilities. These deviations have not been detected.

This method is rather indirect, however, and it cannot be easily employed on primates, which are predominantly single ovulators. Therefore, in order to provide a further basis of support for the biological assumption that nonspatial interactions play the only significant role in follicle growth, we have developed a stochastic model that describes various aspects of the follicular distribution in the presence of only these global growth factors. Our method will be of particular interest in chemical physics because of the nature of the model: we have a polydisperse system of soft spheres which, since there are no local hormonal interactions, can be described by a simple physical potential. The probability of finding the system at a given total potential  $\phi = \phi_0$  is described by the Boltzmann factor, where the system is taken to have some certain biological temperature  $\beta$ .

We base our model on four principal assumptions:

1. The only forces acting on the system are conservative forces due to geometric considerations—the direct contact interactions between bodies—and nonconservative forces due to global growth factors—those which affect only the system as a whole and do not disturb spatial equilibrium. We may therefore describe the state of the system by a physical potential due to the contact forces; the distribution of this potential is given by the Boltzmann factor.

2. The follicles are elastic sacs filled with an incompressible fluid, and therefore act as soft spheres. These spheres are distorted by contact with one another and with the ovary wall. They are also distorted by the rigid connective tissue in the interstitium; this tissue is oriented principally in one direction only,<sup>(24)</sup> so the interstitium distorts the follicles uniformly along one principal axis.

3. A given follicle pair has interaction potential

$$\phi_{ij} = \frac{V_{ij}}{r_{ij}^p} \quad (50)$$

where  $r_{ij}$  is the separation of the two bodies' centers,  $p$  is a parameter of the model, and  $V_{ij}$  is the bodies' "overlapping volume"—the volume that they would share were they to remain as spheres and not be distorted. (A slightly more complicated function determines the potential for interactions between follicles and the ovary wall.) Note that  $\phi_{ij}=0$  in all cases where the two bodies are not distorted at all. Our particular choice of  $\phi_{ij}$  is purely an empirical function that comes from our observations of the follicular distribution and distortions in a sample ovary, and could be improved by a more careful study of the dynamics of fluid-filled sacs.

It is further assumed here that 3-body interactions are not significant and that the total potential  $\phi$  for the system is simply

$$\phi = \sum_{\text{pairs } ij} \phi_{ij} + \sum_i W_i \quad (51)$$

(the  $W_i$  term signifying the contribution from wall interactions).

4. The number of developing follicles  $N$  in the ovary is large. This operational assumption enables us to solve the model numerically by Monte Carlo simulation.

We formalize the assumptions as follows. From assumption 1, we know that the system has a potential  $\phi$ , distributed in the  $3N$ -dimensional space of the follicle positions according to the Boltzmann distribution:

$$P(\phi(\tilde{r}_1, \dots, \tilde{r}_N)) d\tilde{r}_1 \cdots d\tilde{r}_N = \exp[-\beta\phi(\tilde{r}_1, \dots, \tilde{r}_N)] d\tilde{r}_1 \cdots d\tilde{r}_N \quad (52)$$

where the  $\tilde{r}_i$  are the locations of follicle centers. The biological temperature  $\beta$ , like  $p$ , is a parameter of the model. This temperature represents the "stiffness" of the follicles:  $\beta=0$  implies infinitely soft spheres, whereas  $\beta=\infty$  implies completely hard spheres.

From assumption 2, we know that the interstitial tissue imposes a unidirectional distortion; to compensate for this, we apply a certain rescaling factor  $\eta$  in the direction of distortion ( $\eta$  and the direction are determined empirically). The locations  $\tilde{r}_i$  therefore refer to the follicle positions after the system has undergone such a rescaling transformation.

Now, from assumption 3, we know that

$$\begin{aligned} \phi &= \sum_{\text{pairs } ij} \phi_{ij} + \sum_i W_i \\ &= \sum_{\text{pairs } ij} \frac{V_{ij}}{r_{ij}^p} + \sum_i W_i \end{aligned} \quad (53)$$

where  $W_i$ , again, is calculated by a somewhat complicated algorithm involving the ovary wall. To be precise, this algorithm considers the “reflection”  $i'$  of follicle  $i$  about the plane of the wall which cuts through the follicle; then,  $W_i \equiv \phi_{ii'}$ , where  $\phi_{ii'}$  uses the overlapping volume  $V_{ii'}$  and separation  $r_{ii'}$  between the follicle and its “reflection.”

Finally, from assumption 4, we can use a Monte Carlo simulation to solve for quantities predicted by the model. Specifically, we use a modification of the Metropolis algorithm: because of the high packing density of follicles in the ovary, we introduce fluctuations into the system not only through small displacements of follicles, but also through long-range follicle pair exchange.

The model is effected, then, by the following method: the follicles of an observed Rhesus monkey ovary are mixed up according to  $\phi$  and  $P(\phi)$ , and the results are compared with the original observation. In particular, we are interested in comparing the distribution of “larger” and “smaller” follicles between the observed and simulated ovaries, since this is a direct indication of the significance of any local, spatially-dependent forces that may affect follicle growth. If, for instance, there are chemicals secreted by follicles in proportion to follicle size which promote growth at short range only, we might expect to find in the observed ovary a clustering of large follicles that the model would not predict.

We look, specifically, at the probability that a follicle found at a given distance from a typical “large” follicle will itself be “large.” We express this explicitly as

$$q(r) \equiv \frac{n(r)}{n(r) + m(r)} \quad (54)$$

$n(r)$  is defined as the number of pairs  $i, j$  with separation  $d_{ij} = r$ , where  $R_i, R_j > \alpha$  and  $m(r)$  is defined as the number of pairs  $i, j$  with separation  $d_{ij} = r$ , where  $R_i < \alpha < R_j$  or  $R_j < \alpha < R_i$ . Here,  $R_i$  and  $R_j$  are the radii of follicles  $i$  and  $j$  (the radii when the follicles, taken as soft spheres, are undistorted), and  $\alpha$  is the threshold value which divides “large” from “small” follicles. (It is, of course, difficult to define this threshold value precisely, but it should be placed somewhere near the middle of the distribution of follicle sizes, with the many very immature follicles below it and the few nearly mature follicles above it. In our case, we had roughly 75% of the follicles smaller than the threshold and 25% larger than the threshold, but in fact the exact place of the division did not seem to have any great effect on the final results.)  $n(r)$  and  $m(r)$  are pair correlation functions related to the more standard correlation function  $n_{2,\sigma\sigma}(r)$ . Specifically,  $n(r)$  is the number of large-large pairs at separation  $r$ , and  $m(r)$  is twice the number [due to

double counting necessary for the quantity  $q(r)$ ] of large–small pairs at separation  $r$ . Then  $q(r)$  is an average proportion of large follicles at distance  $r$  from a typical large follicle.

In fact, though, we do not measure separation continuously with  $r$ , but rather in discrete “shells”  $k$ , since the follicle sizes are large on the scale of the entire system (there are about 300 tightly packed developing follicles in one ovary—see the cross section in Fig. 10). Instead of (54), we are really interested in

$$q_k \equiv \frac{n_k}{n_k + m_k} \quad (55)$$

$n_k$  is now the number of large–large pairs whose separation lies in the  $k$ th shell, and similarly with  $m_k$ . It is not necessary that these shells  $k$  be placed at regular intervals of  $r$ , but only that each one contain a statistically significant number of follicle pairs, and that there be enough shells to allow good resolution.

The results of the model are currently in the preliminary stages, but although we are still searching for suitable values of the model's



Fig. 10. Digitized image of a 7- $\mu$ m-thick ovarian cross section from a Rhesus monkey on day 4 of the menstrual cycle. This is believed to be the time when the follicle selection process is occurring in this species.

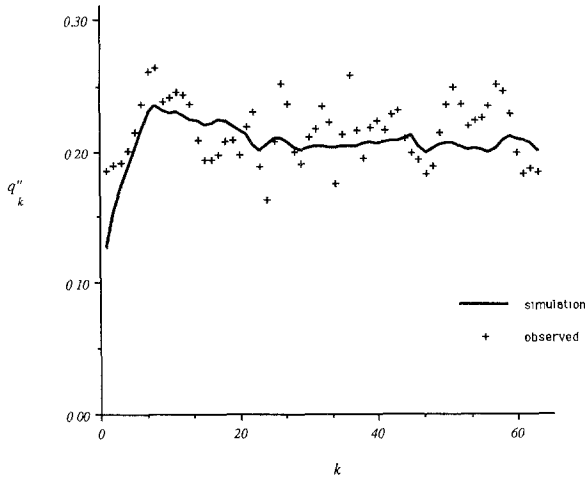


Fig. 11.  $q_k''$  vs.  $k$  for an actual ovary whose typical cross section is shown in Fig. 10 and for the stochastic model with parameters  $\beta = 2.65$  and  $p = 2$ . Here  $\beta$  has units of 1/distance, where distance is measured in digital units of  $17 \mu\text{m}$  each.

parameters, it is instructive to note some of what we have seen so far. Figure 11 shows the statistics for the original follicle distribution and the simulated follicle distribution for  $\beta = 2.65$  and  $p = 2$ . As a noise-reducing algorithm, we average successive points in  $q_k$  vs.  $k$  twice;  $q_k''$  on the ordinate axis is defined as

$$q_k'' \equiv \frac{q_k + 2q_{k+1} + q_{k+2}}{4} \tag{56}$$

The distance between  $k$  and  $k + 1$  is typically between  $15$  and  $35 \mu\text{m}$ , except for the first few shells, which, in order to contain a sufficient number of follicle pairs, are considerably larger (see Table I). By comparison, a typical diameter of the ovary, after the coordinates have been rescaled to compensate for interstitial distortion, is  $5 \text{ mm}$ .

Both the simulated and observed graphs of Fig. 11 show an increase in

Table I

Shell	Radial interval
$k = 1$	$0 < r < 320\mu$
$k = 2$	$320\mu < r < 420\mu$
$k = 65$	$1.952 \text{ mm} < r < 1.968 \text{ mm}$

$q_k''$  at short range (until  $k = 8$ , or  $r \approx 700 \mu\text{m}$ , which happens to be close to the radius of the largest follicle in the ovary), due to the geometrical constraints of interactions through the potential  $\phi$ . The  $(q_k'')$ <sub>observed</sub>, however, is consistently higher than  $(q_k'')$ <sub>simulated</sub>, so under these parameters the model cannot quite account for an unexpectedly high proportion of large follicles near other large follicles. The discrepancy is not great—clustering does not occur to any substantial extent—and we believe that tests under different ranges of parameters will provide better agreement with the observed results. Careful attention is necessary, however, since this region should be very sensitive to the effects of possible spatially-dependent hormonal interactions.

At longer range, furthermore, we see in the observed data what appears to be a periodic packing effect that the model does not clearly predict. This packing effect in a complicated three-dimensional volume such as the mammalian ovary is not well understood, and, while it is at sufficiently long range that it should not be directly relevant to spatially-dependent hormonal interactions, the effect must be investigated more carefully. Tests under new sets of parameters will be informative in this sense as well.

## ACKNOWLEDGMENTS

The authors would especially like to thank Dr. Jerome K. Percus, who has made significant contributions to every aspect of this project. We also acknowledge the many contributions of Dr. C. S. Peskin and Dr. E. Akin. We thank Dr. M. J. Koering for supplying the ovarian sections and Ms. Shirley Hu for entering much of the ovary data and the Courant Institute of Mathematical Sciences for providing much of the technical support in several aspects of the project. Many of the simulations were performed using the NCSA Cray Supercomputing facilities. We wish, finally, to acknowledge the financial support of the Marcus and Bertha Coler Philanthropic Fund.

## REFERENCES

1. A. Lipschütz, New developments in ovarian dynamics and the law of follicular constancy, *Br. J. Exp. Biol.* **5**:283–292 (1928).
2. R. E. Jones, Control of follicular selection, in *The Vertebrate Ovary*, R. E. Jones, ed. (Plenum Press, New York, 1978), Chapter 22, pp. 763–786.
3. N. B. Schwartz, The role of FSH and LH and of their antibodies on follicle growth and on ovulation, *Biol. Reprod.* **10**:236 (1974).
4. A. J. Zeleznik, Premature elevation of systemic estradiol reduces serum levels of follicle stimulating hormone and lengthens the follicular phase of the menstrual cycle in Rhesus monkeys, *Endocrinology* **109**:352–355 (1981).

5. D. T. Baird, R. Horton, D. Longcope, and J. F. Tait, Steroid dynamics under steady state conditions, *Recent Prog. Hormone Res.* **25**:611–664 (1969).
6. C. M. Cargille, G. T. Ross, and T. Yoshimi, Daily variation in plasma follicle stimulating hormone, luteinizing hormone, and progesterone in the normal menstrual cycle, *J. Clin. Endocrinol. Metab.* **29**:12–19 (1969).
7. T. Pedersen, Follicle kinetics in the ovary of the cyclic mouse, *Acta Endocrinol.* **64**:304–323 (1970).
8. L. Speroff and R. L. VandeWiele, Regulation of the human menstrual cycle, *Am. J. Obstet. Gynecol.* **109**:234 (1971).
9. C. C. Tsai and S. S. C. Yen, Acute effects of intravenous infusion of 17 $\beta$ -estradiol on gonadotropin release in pre- and postmenopausal women, *J. Clin. Endocrinol. Metab.* **32**:766–771 (1971).
10. C. M. Tapper and K. Grant-Brown, The secretion and metabolic clearance rates of estradiol in the rat, *J. Endocrinol.* **64**:215–227 (1975).
11. E. Akin and H. M. Lacker, Ovulation control: The right number or nothing, *J. Math. Biol.* **20**:113–132 (1984).
12. H. M. Lacker and E. Akin, How do the ovaries count?, *Math. Biosci.* **90**:305–332 (1987).
13. H. M. Lacker, M. E. Feuer and E. Akin, Cell to cell signalling through circulatory feedback: A mathematical model of the mechanism of follicle selection in the mammalian ovary, in *Cell to Cell Signalling: From Experiments to Theoretical Models*, A. Goldbeter, ed. (Academic Press, London, 1989), pp. 359–385.
14. H. M. Lacker, W. H. Beers, L. E. Meuli, and E. Akin, A theory of follicle selection: I. Hypotheses and examples, *Biol. Reprod.* **37**:570–580 (1987).
15. H. M. Lacker, W. H. Beers, L. E. Meuli, and E. Akin, A theory of follicle selection: II. Computer simulation of estradiol administration in the primate, *Biol. Reprod.* **37**:581–588 (1987).
16. L. E. Meuli, H. M. Lacker, and R. B. Thau, Experimental evidence supporting a mathematical theory of the physiological mechanism regulating follicle development and ovulation number, *Biol. Reprod.* **37**:589–594 (1987).
17. H. M. Lacker, Temporal order and disorder in a model that regulates ovulation number, in *Temporal Disorder in Human Oscillatory Systems*, L. Rensing, U. an der Heiden, and M. C. Mackey, eds. (Springer-Verlag, Berlin, 1986), pp. 248–257.
18. A. McLaren, The distribution of eggs and embryos between sides in the mouse, *J. Endocrinol.* **27**:157 (1963).
19. D. S. Falconer, R. G. Edwards, R. E. Fowler, and R. C. Roberts, Analysis of differences in the number of eggs shed by the two ovaries of mice during natural estrous and after superovulation, *J. Reprod. Fertil.* **2**:418–437 (1961).
20. F. W. Brambell, Reproduction in the common shrew. I. The estrous cycle of the female, in *Philos. Trans. R. Soc. Lond. B Biol. Sci.* **225**:1 (1935).
21. F. W. Brambell and K. Hall, Reproduction in the lesser shrew, *Proc. Zool. Soc. Lond.* **106**:957 (1936).
22. F. W. Brambell and I. W. Rowlands, Reproduction of the bank vole, Vol. 1. The estrous cycle of the female, *Philos. Trans. R. Soc. Lond. B Biol. Sci.* **226**:71 (1936).
23. C. H. Danforth and S. B. de Aberle, The functional interrelation of the ovaries as indicated by the distribution of fetuses in mouse uteri, *Am. J. Anat.* **41**:65 (1928).
24. J. D. Murray, G. F. Oster, and A. K. Harris, A mechanical model for mesenchymal morphogenesis, *J. Math. Biol.* **17**:125 (1983).